

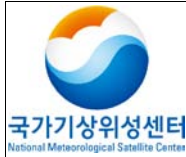
Algorithm Theoretical
Basis Document
For Cloud Optical Thickness

Code:NMSC/SCI/ATBD/COT
Issue:1.0 Date:2012.12.26
File: COP-ATBD_V4.0.hwp
Page : 1/43

COT Algorithm Theoretical Basis Document

NMSC/SCI/ATBD/COT, Issue 1, rev.4

26 December 2012

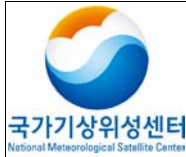


Algorithm Theoretical
Basis Document
For Cloud Optical Thickness

Code:NMSC/SCI/ATBD/COT
Issue:1.0 Date:2012.12.26
File: COP-ATBD_V4.0.hwp
Page : 1/43

REPORT SIGNATURE TABLE

Function	Name	Signature	Date
Prepared by	Yong-Sang Choi, Heaje Cho		26 December 2012
Reviewed by	Yong-Sang Choi		26 December 2012
Authorised by	NMSC		26 December 2012

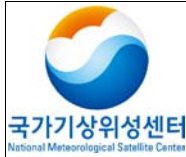


Algorithm Theoretical
Basis Document
For Cloud Optical Thickness

Code:NMSC/SCI/ATBD/COT
Issue:1.0 Date:2012.12.26
File: COP-ATBD_V4.0.hwp
Page : 1/43

DOCUMENT CHANGE RECORD

Version	Date	Pages	Changes
Version5	2012.12.26	-	-Nothing has changed for contents besides ATBD form.

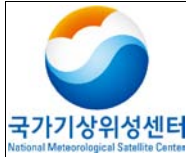


**Algorithm Theoretical
Basis Document
For Cloud Optical Thickness**

Code:NMSC/SCI/ATBD/COT
Issue:1.0 Date:2012.12.26
File: COP-ATBD_V4.0.hwp
Page : 1/43

Table of contents

- 1. Overview**
- 2. Background and purpose**
- 3. Algorithm**
 - 3.1 Theoretical background and basis**
 - 3.2 Retrieval method**
 - 3.3 Retrieval process**
 - 3.4 Validation**
 - 3.4.1 Validation method**
 - 3.4.2 Validation data**
 - 3.4.3 Temporal and spatial collocation method**
 - 3.4.4 Validation result analysis**
- 4. Interpretation method of retrieval result**
- 5. COMS version and algorithm improvement after COMS satellite launch**
- 6. Problems and possibilities for improvement**
- 7. References**



Algorithm Theoretical
Basis Document
For Cloud Optical Thickness

Code:NMSC/SCI/ATBD/COT
Issue:1.0 Date:2012.12.26
File: COP-ATBD_V4.0.hwp
Page : 1/43

List of Tables

Table 1 : Lookup table for COT & ER algorithm.

Table 2 : QC flag.

Table 3 : Definitions of terms used in this analysis.

Table 4 : Validation results of COT

Table 5 : Detailed Output data for the COT algorithm.

Table 6 : Quality test result for the COT algorithm.

List of Figures

Figure 1 : Comparison of ch1 and ch3 radiances for various cloud optical thicknesses and effective radius values (King et al, 1997).

Figure 2 : Sensitivity of SWIR3.7 μm thermal radiances ($L_{3.7}^{\text{sk}}$) to IR10.8- μm satellite-received radiances ($L_{10.8}^{\text{obs}}$) for the clouds with a variety of τ_c (0 to 64) and r_e (0 to 32 μm) under diverse T_c and T_g . The solid line is the 2nd-order polynomial regression line of the plots.

Figure 3 : Simulated radiances in VIS0.65 μm as a function of cloud optical thickness and surface albedo (A_g).

Figure 4 : Flow chart for the cloud detection algorithm.

Figure 5 : The relationships between the radiance at 0.65 and 3.75 μm for various values of cloud optical thickness and effective particle radius.

Figure 6 : JAMI/MTSAT-1R radiance imagery for the five spectral channels centered at 0.725 (VIS), 10.8 (IR1), 12.0 (IR2), 6.75 (IR3), and 3.75 μm (IR4) for 0333 UTC August 7, 2006. Except for the VIS channel, the brighter color corresponds to a relatively low value in $\text{W m}^{-2} \text{sr}^{-1} \text{m}^{-1}$. The full-disk imagery covers East Asia, West Pacific, Australia, and a part of the Antarctic region (80.5S80.5N, 60.4E139.4W).

Figure 7 : Cloud optical thickness and effective radius derived by the CLA from the JAMI level-1b calibrated radiances shown in Figure 1. Base products (left) are the results of conventional methods or without correction methods, and final products (right) from improved methods or with the correction methods developed in the present study.

Figure 8 : Relative frequency (in %) of cloud optical thickness without using the decoupling method (i.e., base products), using the decoupling method (i.e., final products), and MODIS data to the total clouds for the corresponding conditions. SH and NH stand for the Northern and Southern Hemispheres, respectively.

Figure 9 : Same as figure 8 but for cloud effective radius (in μm).

Figure 10 : Same as figure 8 but for base COT using the VIS and IR4 radiances (a), and final COT corrected using the decoupling method in order to have a reflected component from clouds only in the radiances (b).

 <p>국가기상위성센터 National Meteorological Satellite Center</p>	<p style="text-align: center;">Algorithm Theoretical Basis Document For Cloud Optical Thickness</p>	<p>Code:NMSC/SCI/ATBD/COT Issue:1.0 Date:2012.12.26 File: COP-ATBD_V4.0.hwp Page : 1/43</p>
--	---	---

Figure 11: Same as figure 9 but for base ER (a) and final ER (b).

Figure 12 : Relative frequency of MTSAT minus MODIS COT/ER for the maximum values. Errors in the retrieved COT/ER (in %) with respect to the corresponding parameters. The solid and dotted lines indicate values from the final (corrected) and base (uncorrected) products, respectively.

Figure 13 : Modified COT code for removing land-sea discontinuities.

Figure 14 : Cloud optical thickness (a)before and (b)after correcting program code at 15th, Nov, 2011.

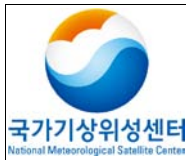


Algorithm Theoretical
Basis Document
For Cloud Optical Thickness

Code:NMSC/SCI/ATBD/COT
Issue:1.0 Date:2012.12.26
File: COP-ATBD_V4.0.hwp
Page : 1/43

List of Acronyms

COMS	Communication, Ocean, and Meteorological Satellite
MTSAT	Multi-functional Transport Satellite
JAMI	Japanese Advanced Meteorological Imager
ISCCP	International Satellite Cloud Climatology Project
SOBS	Gridded surface weather station reports
FOV	Field of view
MODIS	Moderate Resolution Imaging Spectroradiometer
COT	Cloud Optical Depth
ER	Effective Radius
SBDART	Santa Barbara DISORT Atmospheric Radiative Transfer



Algorithm Theoretical Basis Document For Cloud Optical Thickness

Code:NMSC/SCI/ATBD/COT
Issue:1.0 Date:2012.12.26
File: COP-ATBD_V4.0.hwp
Page : 1/43

1. Overview

This algorithm is to retrieve cloud optical thickness (COT) and Effective particle radius. Input data was retrieved using the radiance of VIS $0.65\mu\text{m}$ and SWIR $3.75\mu\text{m}$. It is possible for this algorithm to retrieve of cloud optical thickness on characteristic of $0.6\mu\text{m}$ channel in the daytime. VIS $0.65\mu\text{m}$ is influenced by surface reflectance. Surface reflectance is important in the retrieval of cloud optical thickness and effective particle radius. SWIR $3.75\mu\text{m}$ in the daytime includes terrestrial radiation. We use IR $10.8\mu\text{m}$ radiance to eliminate it. The corrected VIS $0.65\mu\text{m}$ and SWIR $3.75\mu\text{m}$ radiance simultaneously obtain the optimal cloud optical thickness and effective particle radius consistent with the previously calculated Look-up table using the Radiative Transfer Model (RTM). The retrieved information is essential not only to the study of cloud radiative forcing, but also for classifying ISCCP cloud types.

2. Background and purpose

The COT algorithm is performed for daytime cloud pixels. Therefore, Sun Zenith angle and scene analysis tests are needed. This is achieved using previously calculated results. This includes radiance of IRIR $10.8\mu\text{m}$ and the surface reflectance in the algorithm. For VIS $0.65\mu\text{m}$, it is affected by the surface reflectance, so a correction is needed. The correction is calculated by a simple function. A constant function was designed to change depending on the surface reflectance. The surface reflectance value used in the algorithm is calculated using high resolution MODIS Terra and Aqua albedo data for spatial resolution in eight day intervals. SWIR $3.75\mu\text{m}$ simultaneously includes thermal radiation and solar radiation. It is modified to process as function of IR $10.8\mu\text{m}$ brightness temperature of earth radiation component. The final product using calculated and observed value of LUT retrieves simultaneously cloud optical thickness and effective particle radius.

3. Algorithm

3.1 Theoretical background and basis

GMS-5, retrieves cloud optical thickness using only the visible channel. This method assumes an effective particle radius of $10\mu\text{m}$ in all clouds. The improved cloud optical thickness algorithm by



Algorithm Theoretical
Basis Document
For Cloud Optical Thickness

Code:NMSC/SCI/ATBD/COT
Issue:1.0 Date:2012.12.26
File: COP-ATBD_V4.0.hwp
Page : 1/43

thereafter King (1987) and Nakajima et al. (1990) developed solar reflectance technique. This method retrieves in the daytime at a spatial resolution of 1km by the current MODIS.

This algorithm used a solar reflectance technique similar to MODIS. The solar reflectance technique uses the visible and SWIR channels. It can classify two types depending on the absorption or non-absorption of water vapor as follows:

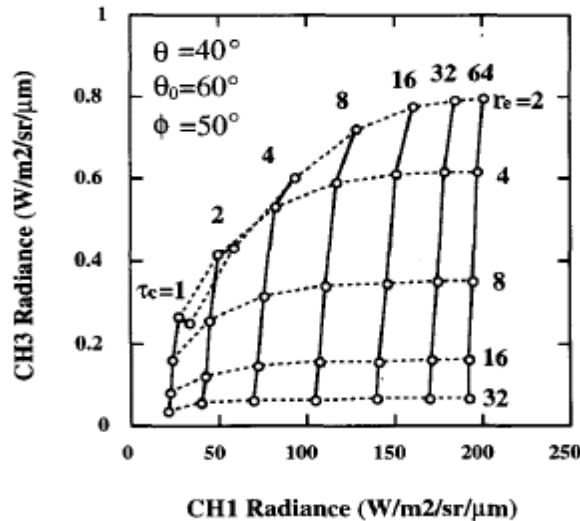
- a. Water vapor non-absorbing region : 0.65, 0.86, 1.24 μm
- b. Water vapor absorbing region : 1.6, 2.1, 3.7 μm

In addition, non-absorbing wavelength range of water vapor by properties of surface uses as follows:

- a. Land : 0.65 μm , Ocean : 0.86 μm
- b. Snow/ Ice : 1.24 μm

Fig. 1 graphs the Solar reflected radiance of AVHRR channel 1 (0.64 μm) and channel 3 (3.75 μm) as a function of cloud optical thickness ($\tau_c = 1, 2, 4, 8, 16, 32, 64$) and effective particle radius ($r_e = 2, 4, 8, 16, 32$). Thus, the reflectance for absorbing wavelength and non-absorbing wavelength of water vapor depends upon the size of cloud optical thickness and effective particle radius. The reflectance of two regions are calculated beforehand via the Radiative Transfer model to find out the optimal cloud optical thickness and effective particle radius consistent with observation values. More detailed content can be found in pages 4,722-4,725 of the Appendix (Choi et al. 2007, IJRS).

Fig. 1. Comparison of ch1 and ch3 radiances for various cloud optical thicknesses and effective radius values (King et al, 1997).



Data retrieval during the daytime with current technology is possible. It is applied to water phase cloud, but the results are uncertain due to retrieval problems with cirrus clouds. All three 0.65, 0.86, and 1.24 μm channels are required in the non-absorbing wavelength of water vapor for the earth's surface. However, the SWIR region requires only one of 1.6 μm or 3.75 μm in the absorbing wavelength of water vapor. This COMS algorithm retrieves cloud optical thickness over land and oceans using the available 0.675 μm , Surface covered in ice and snow were not considered. The current ISCCP defines cloud optical thickness as reflectance of 0.6 μm . It can produce the minimum necessary data for ISCCP cloud type classification. If the coefficients of the Radiative Transfer Model are not properly selected, the exact LUT is difficult to obtain.

3.2 Retrieval method

3.2.1. LUT retrieval method

<pre>##### # SBDART input program for COT lookup table ##### if [\$do4] ; then rm -f \$root.4 echo running example 4</pre>	<p>Do-loop start!</p>
--	-----------------------



Algorithm Theoretical
Basis Document
For Cloud Optical Thickness

Code:NMSC/SCI/ATBD/COT
Issue:1.0 Date:2012.12.26
File: COP-ATBD_V4.0.hwp
Page : 1/43

<pre> for albcon in 0 0.5 ; do for tcloud in 0 2 4 8 16 32 64 128; do for nre in -2 -4 -8 -16 -32 -64; do for sza in 0 10 20 30 40 50 60 70 80 ;do echo " &INPUT albcon=\$albcon tcloud=\$tcloud sza=\$sza nre=\$nre wlinf=0.73 wlsup=0.73 uzen=0,10,20,30,40,50,60,70,80 phi=0 idatm=2 iout=20 nothrm=1 /" > INPUT sbdart>> \$root.4 done done done done fi </pre>	<p>A spectrally uniform, surface albedo cloud optical thickness effective radius (positive=water, negative=ice) solar zenith angle</p> <p>surface albedo cloud optical thickness solar zenith angle effective radius lower wavelength limit upper wavelength limit satellite zenith angle</p> <p>idatm = 1 for tropical = 2 for mid-latitude summer = 3 for mid-latitude winter</p> <p>Radiance output at TOA km 1 for no thermal emission</p>
--	--

Cloud optical thickness and effective particle radius is a function of reflectance in the absorbing and non-absorbing wavelengths of water vapor. We retrieved the optimal cloud optical thickness and effective particle radius consistent with observation values for beforehand calculated reflectance in the Radiative Transfer model using this principle. This has a variety of input conditions of surface

reflectance, cloud optical thickness, effective particle radius, sun zenith angle, and satellite zenith angle. This was performed using the SBDART RTM for the tropics, and the mid-latitudes in the summer and winter. In $0.65 \mu\text{m}$ surface reflectance is influenced by the thermal radiation of $3.75 \mu\text{m}$ and must consider this correction.

Reflectance is also different depending on the geometric observation angle and the sun incident angle and must take these factors into consideration (Table 1). Table 1 presents the LUT to retrieve cloud optical thickness. θ_0 is the sun zenith angle, θ is the satellite zenith angle. LUT is calculated simply for rearranging of array in IDL program. The input data of the IDL program is the simulated $3.75 \mu\text{m}$, $0.675 \mu\text{m}$ radiance for a variety of simulated COT and CR through the SBDART.

Table 1. Lookup table for COT & ER algorithm.

Land/Sea	θ_0	θ	Rad0.6	Rad3.7	COT	ER
0	35	23	0.12	0.23	45.23	3.23
1	34	23	0.11	0.22	23.42	12.32
0	21	45	0.34	0.45	84.12	21.31
...

SWIR $3.75 \mu\text{m}$ daytime radiance simultaneously includes thermal radiation and solar radiation. Therefore, for retrieval of cloud optical thickness, $3.75 \mu\text{m}$ thermal radiance must be removed to improve accuracy. In order to remove the thermal radiation, we used $10.8 \mu\text{m}$ radiance. Fig. 2 presents the relationship between $10.8 \mu\text{m}$ radiance and $3.75 \mu\text{m}$ thermal radiation.

We removed $3.75 \mu\text{m}$ thermal radiation using the relationship for Cloud optical thickness retrieval. VIS $0.65 \mu\text{m}$ radiance is a function of cloud optical thickness and surface albedo. We simulated a change of VIS $0.65 \mu\text{m}$ radiance depending on surface reflectance in a variety of conditions (solar zenith angle: $0 \sim 80$, solar zenith angle: $0 \sim 80$, cloud optical thickness: $0 \sim 123$, effective particle radius: $2 \sim 64$) using the Radiative Transfer Model. The effect of surface reflectance can be expressed by the following simple function:

$$L_{0.65} = a_0 + a_1 L_{0.65}^{\text{obs}} + a_2 (L_{0.65}^{\text{obs}})^2 \quad (1)$$

$L_{0.65}$ is the corrected VIS $0.65\mu\text{m}$ radiance, and $L_{0.65}^{\text{obs}}$ is the satellite-observed VIS $0.65\mu\text{m}$ radiance. a_0 , a_1 , and a_2 are regression coefficients. They depend on the surface reflectance. As a result, to removal of surface reflectance in cloud optical thickness retrieval can directly influence the accuracy of the product.

Fig. 2. Sensitivity of SWIR3.7 μm thermal radiances ($L_{3.7}^{\text{th}}$) to IR10.8- μm satellite-received radiances ($L_{10.8}^{\text{obs}}$) for the clouds with a variety of τ_c (0 to 64) and r_c (0 to $32\mu\text{m}$) under diverse T_c and T_g . The solid line is the 2nd-order polynomial regression line of the plots.

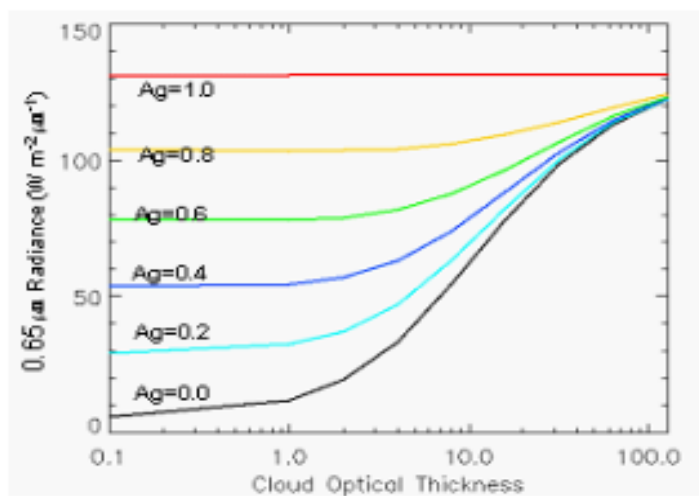
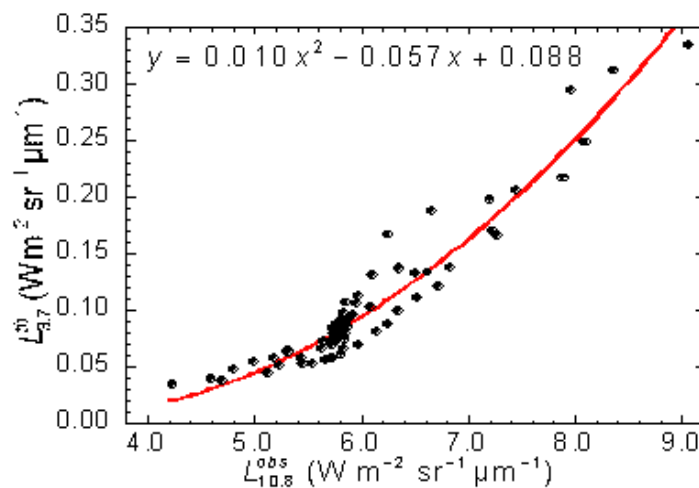
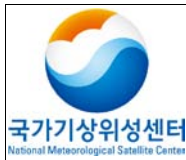


Fig. 3. Simulated radiances in VIS $0.65\mu\text{m}$ as a function of cloud optical thickness and surface albedo (A_g).



Algorithm Theoretical
Basis Document
For Cloud Optical Thickness

Code:NMSC/SCI/ATBD/COT
Issue:1.0 Date:2012.12.26
File: COP-ATBD_V4.0.hwp
Page : 1/43

3.3 Retrieval process

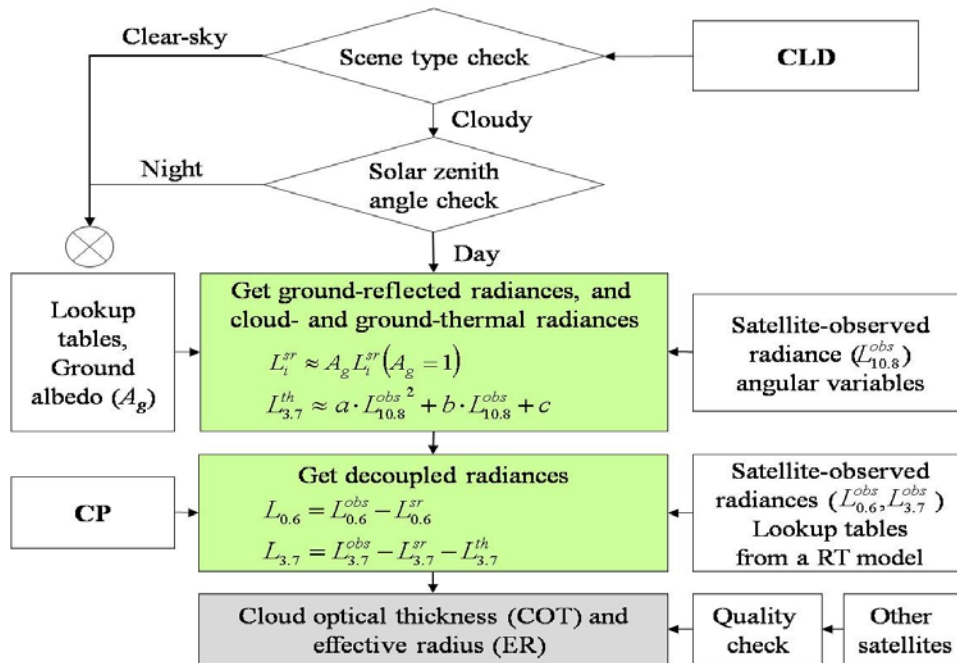
3.3.1 Cloud optical thickness retrieval

The flowchart of the algorithm to get cloud optical thickness is shown in Fig. 4. It applies the algorithm in case of daytime cloud pixels using scene analysis and sun zenith angle test results. The first step of the algorithm corrects VIS $0.65\mu\text{m}$ and SWIR $3.75\mu\text{m}$ by examining the radiance of IR $10.8\mu\text{m}$ and surface reflectance. VIS $0.65\mu\text{m}$ radiance correction uses surface reflectance. SWIR $3.75\mu\text{m}$ radiance correction uses IR $10.8\mu\text{m}$ radiance.

The next step is to simultaneously retrieve cloud optical thickness and effective particle radius of the final product consistent with the calculated value of LUT with the corrected VIS $0.65\mu\text{m}$ and SWIR $3.75\mu\text{m}$ radiance. This step requires cloud phase information. The radiance of VIS $0.65\mu\text{m}$ and SWIR $3.75\mu\text{m}$ are influenced by cloud phase.

LUT was calculated while considering cloud phase information (ice phase, water phase), sun zenith angle ($0\sim 80^\circ$), satellite zenith angle ($0\sim 80^\circ$), and surface reflectance (0,0.5). This algorithm used the surface reflectance of 0.5 instead of 1 suggested by Choi et al. (2007) because real surface reflectance observed in field of view from MTSAT is smaller than 0.5. If it is very small and generates complicated reflectivity between Surface and high level, surface radiance shows a linear relationship with surface reflectance. Sun zenith angle and satellite zenith angle in case of $60\sim 80^\circ$ are rarely a linear relationship. This is a limitation of retrieving cloud optical thickness and effective particle radius.

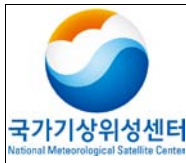
Fig. 4. Flowchart of the COT algorithm.



The SWIR 3.75 μm channel simultaneously receives the solar radiation and daytime thermal radiance effect of daytime (Fig. 5). Fig. 5 a) is not a case of thermal radiation component of SWIR 3.75 μm and Fig. 5 b) included. The difference of these affects the accuracy of the algorithm product. Effectively removing the SWIR 3.75 μm thermal radiance has relevance to the accuracy of the product. The algorithm removed this using the IR 10.8 μm channel. IR10.8 μm is affected only by thermal radiation, it will understand degree of thermal radiation using one. The simple function is established a simple function between the thermal radiation of SWIR 3.75 μm and the radiance of IR 10.8 μm in the simulated results

The thermal radiation component was removed in the radiance of SWIR 3.75 μm observed from satellite using the algorithm applying this function.

Fig. 5. The relationships between the radiance at 0.65 and 3.75 μm for values of cloud optical thickness and effective particle radius.



**Algorithm Theoretical
Basis Document
For Cloud Optical Thickness**

Code:NMSC/SCI/ATBD/COT
Issue:1.0 Date:2012.12.26
File: COP-ATBD_V4.0.hwp
Page : 1/43

	96	0.9~1
4-3 (Optical Depth Range)	12 8 4 0	0 < COT <= 50 50 < COT < 100 COT > 100 COT = 0
2 (Cloud Phase)	3 2	CP = 1 and ER > 30 CP = 2 and ER < 5
1 (ER=>unavailable)	1	ER in detectable range

3.4 Validation

3.4.1 Validation method

The cloud optical thickness retrieved from CMDPS is validated through a variety of methods by the developer. It is a real-time validation of CMDPS and validity of algorithm using MODIS data. CMDPS performed statistical validation to judge the accuracy and validity of the algorithm. The validation by developer is based on scene analysis and climate value. Effective particle radius is retrieved, but a target of validation was excluded.

3.4.1.1. Pre-processing for validation-Simplified ISCCP cloud detection

We used as a input data of algorithm for calibrated radiance and brightness temperature of a hourly Full-disk provided from JAMI sensor on board MTSAT same as simulated images of COMS. The central wavelength of the five channels from JAMI are; 0.725 μm (VIS), 10.8 μm (IR1), 12.0 μm (IR2), 6.75 μm (IR3), and 3.75 μm (IR4). Pre-processing distinguishes clear pixels between clouds and clear in order to validate the needed cloud information product.

The cloud detection algorithm played this role in the CMDPS algorithm, but this validation utilized simplified cloud detection techniques (Rossow and Garder 1993a) of the International Satellite Cloud



Algorithm Theoretical
Basis Document
For Cloud Optical Thickness

Code:NMSC/SCI/ATBD/COT
Issue:1.0 Date:2012.12.26
File: COP-ATBD_V4.0.hwp
Page : 1/43

Climatology Project (ISCCP). For cloud detection, ISCCP uses the spectral test of VIS and IR channels as follows:

Clear: $(BT_{IR1}^{clr} - BT_{IR1}) \leq IRTHR$ and $(L_{VIS} - L_{VIS}^{clr}) \leq VISTHR$

Cloudy: $(BT_{IR1}^{clr} - BT_{IR1}) > IRTHR$ or $(L_{VIS} - L_{VIS}^{clr}) > VISTHR$ (2)

BT_{IR1}^{clr} , BT_{IR1} , L_{VIS} , and L_{VIS}^{clr} are IR1 brightness Temperature in all sky, IR1 brightness temperature in clear sky, radiance of VIS in all sky, and radiance of VIS in clear sky, respectively. L_{VIS} is the adjusted radiance by the percent ratio, which is the same as in the ISCCP algorithm. IRTHR of threshold value is 12.0 K, VISTHR is 6.0% for the land, and 3.0 for the ocean.

The availability of cloud detection has to consider to deciding mainly by the accuracy of the clear sky radiance (Rossow and Garder 1993b). In this validation, BT_{IR1}^{clr} (L_{VIS}^{clr}) set the maximum (minimum) value for each UTC in the month of August, 2006. VISTHR has the same value as ISCCP, because the calculated brightness temperature of IR clear sky is high. IRTHR is 6K higher for land, and 1K higher for oceans than the value suggested by Rossow and Garder (1993a). Therefore, the selection of cloud pixels is stricter than the ISCCP algorithm. It uses only IR condition of equation (2) in nighttime.

The detected cloud amount by the above method accounts for the average CA for August, 2006 about 57.3 % in the JAMI Field Of View (FOV). This value is comparable with estimated results of other global CA climate data. According to Rossow et al. (1993) method, estimated at 62.7% in ISCCP C2 (1984-1988), at 61.2% in Gridded surface weather station reports (SOBS) (1971-1981), at 61.4% in METEOR (1976-1988), and at 51.8% in Nimbus-7 (1980-1984).

One point of notice is higher than JAMI cloud amount. The MODIS cloud amount has an average of 77.6%. It has 18 bands from MODIS in narrower Field of View (FOV), because it detects various clouds, including thin cirrus. Therefore, the results of cloud detection by this method will contain a considerable uncertainty as compared with reality. It is obvious that have cloud information product or uncertainty using above method is obvious. However, thin clouds overlooked by the above simplified cloud detection method is thought to relatively have little influence in the cloud optical thickness and effective particle radius.



**Algorithm Theoretical
Basis Document
For Cloud Optical Thickness**

Code:NMSC/SCI/ATBD/COT
Issue:1.0 Date:2012.12.26
File: COP-ATBD_V4.0.hwp
Page : 1/43

3.4.1.2. Explanation of validation method

Validation is performed for Full-disk JAMI images in the month of August, 2006. This period is decided to consider for the limited time, but Field of view (FOV) of this period includes all situations that have the surface, cloud type, vertical distribution of atmospheric gas, observation and sun zenith angle affecting detection from geostationary satellites. In addition, during this period typhoons Saomi and Bopha reached the Korean Peninsula and Japan. The main purpose of COMS is to predict heavy weather, so this validation period is optimal to examine the performance capacity of the algorithm.

In this validation, cloud products of two type were improved the current version in comparison/validation with “base product” retrieved by traditional algorithm and the “final product“ of the current version algorithm with independently developed by Prof. Chang-Hoi Ho team in Seoul National University.

Basic cloud optical thickness and effective particle radius were retrieved and don't use the decoupling method (Choi et al. 2007). Final cloud optical thickness and effective particle radius were retrieved using the decoupling method. Finally, basic cloud top height was retrieved using radiance of the IR1 channel. The designations of each product used in this validation are summarized in Table 1.

Table 3. Definitions of terms used in this analysis.

Term	Unit	Definition
Base COT/ER	unitless/m	Cloud optical thickness and effective radius are roughly retrieved by using measured VIS and IR4 radiances that remain to include both thermal and reflected components.
Final COT/ER	unitless/m	Cloud optical thickness and effective radius are retrieved by the sun reflection method that uses the decoupled radiances, i.e. cloud-reflected components.

As pointed out above, the defined base, final, and MODIS products compared as four procedures. All of four results correct the algorithm in optimal conditions, and provides useful data to comprehend the weak points.

(1) Scene analysis



Algorithm Theoretical Basis Document For Cloud Optical Thickness

Code:NMSC/SCI/ATBD/COT
Issue:1.0 Date:2012.12.26
File: COP-ATBD_V4.0.hwp
Page : 1/43

Scene analysis is the first activity to be validated. Scene analysis is a comparison between radiance and product. It can review the total reliability of the product.

(2) Climate data comparison

Comparison with climate data is done to identify whether the product is reliable climate data. Also, product data can figure out its bias. Long term data must be obtained, but this validation was limited to August, 2006. Climate data can figure out the cause of bias for retrieval value divided and compare it to a variety of conditions. For example, It compares MODIS product climate data for day, night, water phase cloud, ice phase cloud, southern hemisphere, northern hemisphere, Antarctic region, the tropic region, and the mid-latitude region.

(3) Time-series comparison

Time-series comparison is an activity to compare the ancillary validation data and diurnal variation during a validation period for regions of interest. The region selected are divided between the land, ocean, desert, snow/ice and various surface conditions, low, middle, and high latitudes. The regions selected for this validation are; Seoul, Hwabuk plain in China, the Gobi desert, the Tibetan plateau, the South China Sea, the East Pacific, the Bering Sea, and the Antarctic region.

(4) pixel comparison

Finally, we examine the error range in comparison with ancillary data into pixel units for cloud information product.

In this validation, MODI06 collocation 5 cloud data was used as ancillary data. The validation region for pixel comparison was limited to the Pacific Northwest (10° - 30° N, 113° - 149° E).

A lot of cyclonic eddies of this region have a strong wind and zone of spiral precipitation. A variety of cloud phase is observed from well-developed convective activity (Kim et al. 2006). To avoid a temporal and spatial discrepancy between MODIS and JAMI images, it compared the optimal pixels within 50 km distance and 30 minutes between two images considering the path of wind. About 2,160,000 cloud pixels under this condition were used for the validation. The JAMI pixel resolution is same. The difference of resolution between the two image pixels can lead to uncertainty of results.

3.4.2 Validation data

(1) CMDPS Validation



Algorithm Theoretical Basis Document For Cloud Optical Thickness

Code:NMSC/SCI/ATBD/COT
Issue:1.0 Date:2012.12.26
File: COP-ATBD_V4.0.hwp
Page : 1/43

The data used to validate CMDPS cloud top height is performed using data from November 1 to November 5 of MODIS Terra and Aqua. We calculated the statistical value separated by latitude (the equator: below latitude 30°, mid-latitude: north-south 30~60°). This is the same with other cloud analysis data. In thick cloud optical thickness and high sun zenith angle, inaccuracy rises. In case of cloud optical thickness have greater and less than 16, and it retrieved the statistics value depending on sun zenith angle. Cloud phase and effective particle radius validation was also performed.

(2) Developer validation

Japanese Advanced Meteorological Imager (JMAI) radiance and the spatial resolution of the observation angle used for validation is 4km. Full-disk image is similar to the location of COMS including East Asia, the Western Pacific, Australia, and the Antarctic region. We used MODIS cloud data to compare with products retrieved using JAMI images. This data includes 5km cloud phase resolution for nadir (Platnick et al. 2003). This is more improved point than the previous version in collection 5 data. It is found from other references (Baum et al. 2005, King et al. 2006, Yang et al. 2007). MODIS granules (5-min data) were collocated for the Pacific Northwest (10°-30°N, 113°-149°E) during the period 5-11 August 2006. Cloud optical thickness and effective particle radius of MOD06 is a representative value for the whole atmospheric column decided in using simultaneous visible and NIR channels (0.6, 0.8, 1.2, 2.1 μm). The minimum retrieval range of MOD06 cloud optical thickness is 0.1 (Choi et al. 2005) and The maximum retrieval range is up to 100.

In the case of the effective particle radius, the valid retrieval range is 2-30 μm in liquid phase clouds, and 5~90 μm in ice phase clouds. The two products are retrieved to two decimal places. To compare MODIS data, these CMDPS products were retrieved within the same range. Daily atmospheric data (MOD08, collocation 5) of MODIS gridded level-3 is collocated for the same validation period. MOD08 has a value of 1° per pixel and is calculated by MOD06. MOD08 is the mean value cloud retrieval information during the period of validation, but it is used separately to analyze the time-series analysis for a given grid.

3.4.3 Temporal and spatial collocation method

(1) CMDPS Validation CMDPS

We collocated time and space using data within the range of -8 to 30 minutes on the same method

as the validation of other cloud analysis algorithm. High latitude (above 60° south and north) was excluded from the validation. We excluded from the validation to represent the difference of more than 1-standard deviation in 5x5 pixels of MODIS.

(2) Developer validation

In the case of pixel comparison, CMDPS CLA criteria, it is collocated to averaged temporal and spatial pixels and entering within 30 minutes.

3.4.4 Validation result analysis

(1) CMDPS validation

Table 4. Validation results of COT

	Reference	Time	Region	R	Bias	RMSE
COT	MOD	11/1~11/5	Global	0.73	2.16	3.32
			Low	0.73	1.98	3.05
			Mid	0.68	2.79	3.97
			COT < 16	0.62	2.18	2.84
			COT > 16	0.84	-0.23	19.04
			SOA <30	0.73	2.05	3.36
			SOA >30	0.65	2.27	3.18
			Water	0.54	2.02	2.85
			Ice	0.82	2.77	4.61
	MYD	11/1~11/5	Global	0.90	1.71	3.57
			Low	0.93	1.63	3.79
			Mid	0.66	1.92	2.85
			COT < 16	0.58	1.86	2.57
			COT > 16	0.79	-21.90	31.57
			SOA <30	0.76	1.43	4.35
			SOA >30	0.83	1.84	2.99
Water	0.52	1.61	2.45			

	Algorithm Theoretical Basis Document For Cloud Optical Thickness	Code:NMSC/SCI/ATBD/COT Issue:1.0 Date:2012.12.26 File: COP-ATBD_V4.0.hwp Page : 1/43
---	---	---

			Ice	0.96	2.12	6.18
--	--	--	-----	------	------	------

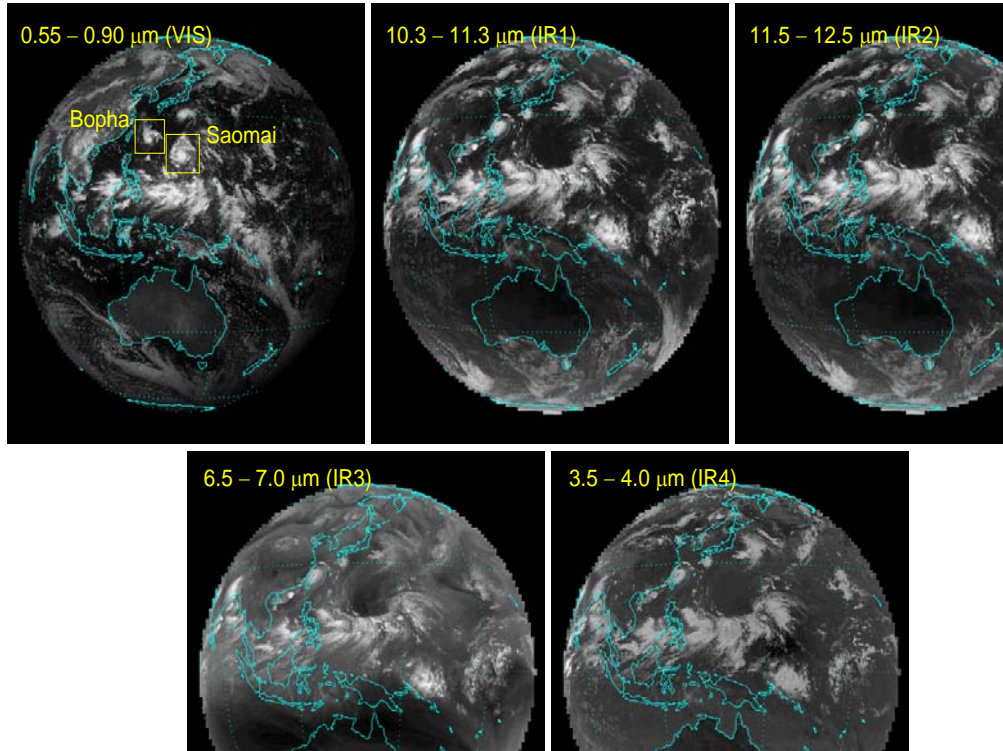
Table 4 shows the results of validation from November 1 to 5, 2008. As mentioned earlier, it shows the statistics value of the correlation coefficient, bias, and RMSE of MODIS and CMDPS cloud optical thickness through a variety of validation conditions.

(2) Developer validation

1) Scene analysis

Fig. 6 is an example of JAMI radiance imagery at 0333 UTC August 7, 2006. Clouds clearly show along the Intertropical convergence zone (ITCZ). Optically thick clouds show brightly by scattering sunlight in VIS images. Clouds above dark surfaces such as oceans are discriminated easily. A bright color in IR image corresponds to relatively low value, and high altitude clouds are bright, because they emit a lower IR radiance from top of clouds. High clouds more than 400 hPa in IR3 images only show brightly. This is because water vapor absorption happens in middle to low level troposphere. Low clouds in IR window channels such as IR1 or IR2 are clearly confirmed. IR4 radiance has a high value in general for small cloud particles, and water phase particles.

Fig. 6. JAMI/MTSAT-1R radiance imagery for the five spectral channels centered at 0.725 (VIS), 10.8 (IR1), 12.0 (IR2), 6.75 (IR3), and 3.75 μ m (IR4) for 0333 UTC August 7, 2006. Except for the VIS channel, the brighter color corresponds to a relatively low value in $W m^{-2} sr^{-1} m^{-1}$. The full-disk imagery covers East Asia, West Pacific, Australia, and a part of the Antarctic region (80.5S80.5N, 60.4E139.4W).



When considering the spectral properties of the 5 images above, this time image is characterized by three great regions based on inferred cloud properties.

(i) High clouds including clouds of Typhoon in the tropic western pacific region and optically thick clouds.

(ii) High clouds of Eastern pacific region and thin clouds

(iii)) An extensive distributed region contains low and thin clouds, high and thick clouds over south-west ocean of Australia

(i) is inferred from high VIS, low IR1, low IR2 radiance, (ii) low VIS, low VIS, low IR2 radiance, (iii) extensively distributed low VIS, high IR1, high IR2 radiance and high VIS, low IR3 of spatial dendrite. We compared the inferred three properties of clouds and CMDPS algorithm products. Here we must review all cloud information.

Fig. 7. Cloud optical thickness and effective radius derived by the CLA from the JAMI level-1b calibrated radiances shown in Figure 1. Base products (left) are the results of conventional methods or without correction methods, and final products (right) from improved methods or with the correction methods developed in the

present study.

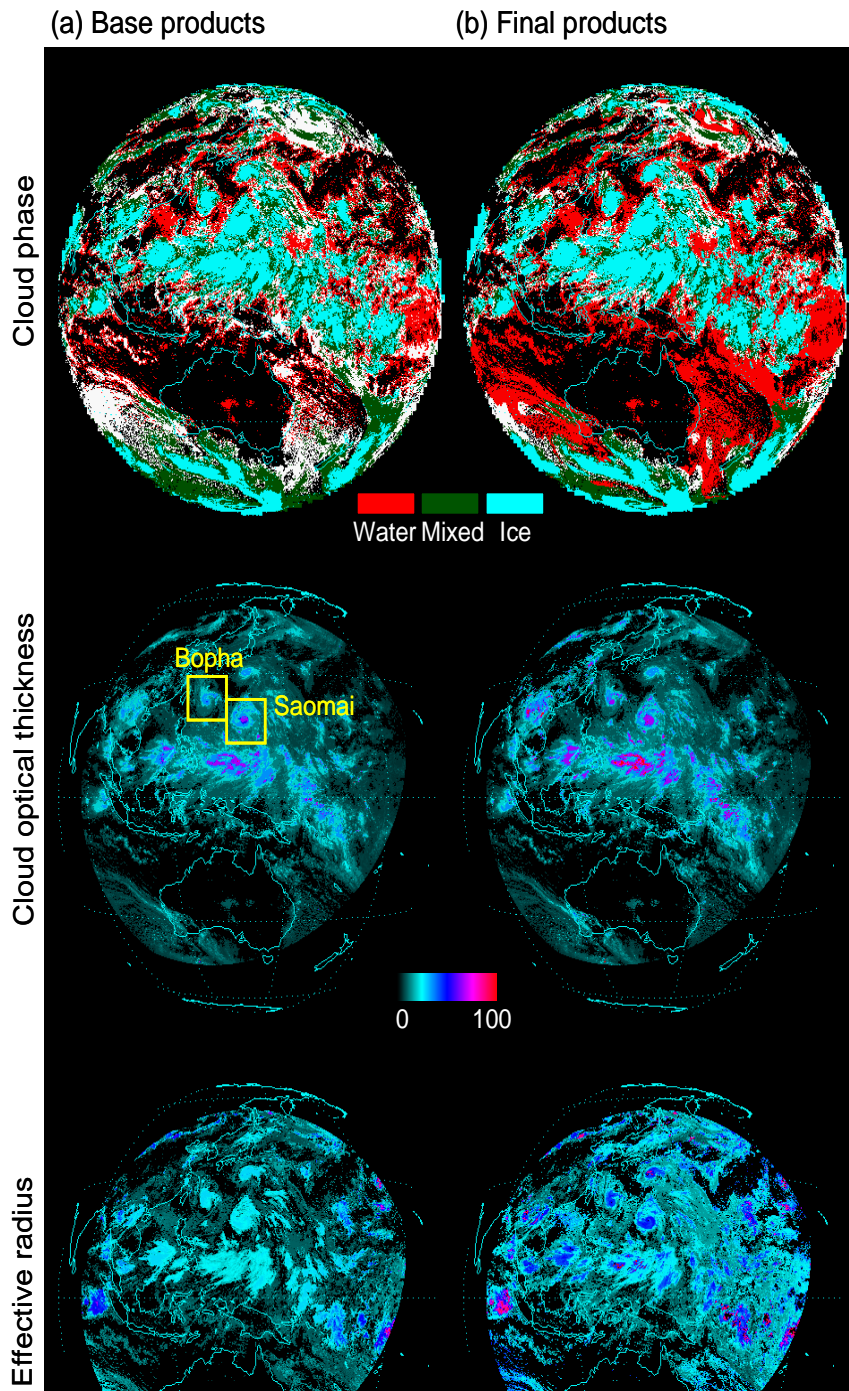
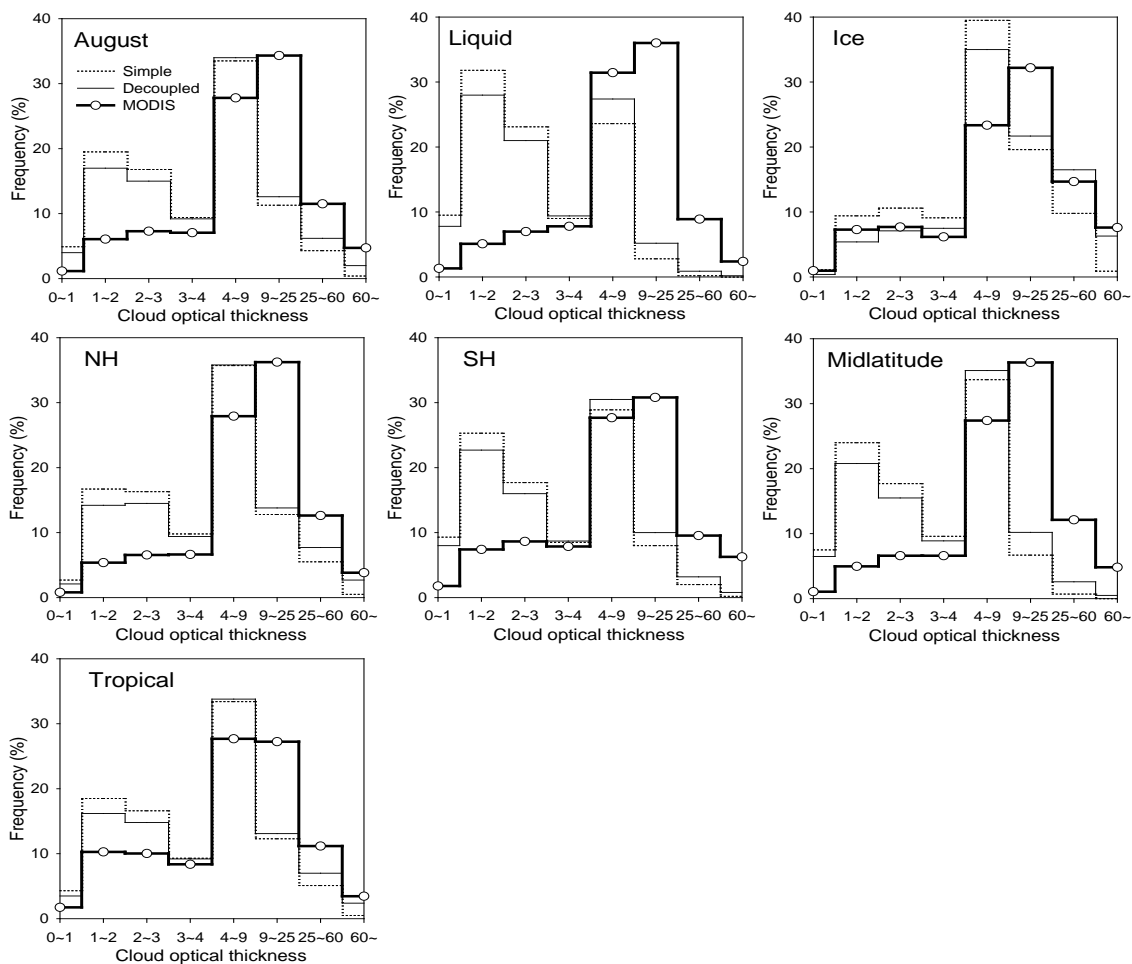


Fig. 8 is a basic product (left) and final product (right) of cloud optical thickness and effective particle radius. There is a clear difference between the two products. The final product represent the

main properties better than the base product. Final cloud optical thickness (Effective particle radius) has a greater value than the base product in ITCZ and typhoons. Very high and thick clouds in the final product is more distinct in the Western Pacific. We cannot estimate cloud optical thickness for high observation angle over than 60° , but the final cloud optical thickness shows the properties of the high and thin clouds of the Eastern Pacific, and high and thick ones near Australia.

2) Comparison of Climate data

Fig. 8. Relative frequency (in %) of cloud optical thickness without using the decoupling method (i.e., base products), using the decoupling method (i.e., final products), and MODIS data to the total clouds for the corresponding conditions. SH and NH stand for the Northern and Southern Hemispheres, respectively.



We showed relative frequency monthly climate data under a variety of conditions(fig. 8)..

The interval of the horizontal axis value is based on criteria of cloud optical thickness for classification



Algorithm Theoretical
Basis Document
For Cloud Optical Thickness

Code:NMSC/SCI/ATBD/COT
Issue:1.0 Date:2012.12.26
File: COP-ATBD_V4.0.hwp
Page : 1/43

of ISCCP cloud type (Rossow and Schiffer 1999).

. The dotted line, solid line, and bold line show the basic, final, and MODIS product. Generally, The retrieved cloud optical thickness is underestimated than MODIS. Both Final and MODIS products have high values in 4~6 and 9~25 of cloud optical thickness. The cloud optical thickness pixels below 4 are less frequent in MODIS, but the frequency of cloud optical thickness pixels between 9 and 5 are more frequent in MODIS. This consistent bias is caused by calculating of model. It may be minimized by tuning the look-up table.

The difference between MODIS and our product is caused by reflective differences of water phase and ice phase clouds. The difference is greater in the water phase than in the ice phase. In Fig. 8, more solar light is reflected by liquid water than by ice particles. As a result, radiance reflected from water phase clouds is greater than radiance reflected from ice phase clouds for the same optical thickness. Due to this property, the cloud information retrieval algorithm can underestimate cloud optical thickness if ice phase clouds are incorrectly detected as water phase clouds. Therefore, cloud phase plays an important role in the accuracy of cloud optical thickness retrieval. We carried out similar analysis for effective particle radius (Fig. 9).

The value produced by our algorithm was slightly underestimated than the corresponding MODIS values. However, the difference is smaller than that for cloud optical thickness. Effective particle radius is small in the water phase, and is big in the water phase both two products. Water phase particles are 2~30 μm and ice particles are 5~60 μm . The highest frequency of water phase is 10~20 μm , and 20~30 μm for the ice phase. There is only a slight difference between the Northern and Southern hemispheres in the effective particle radius. The difference with MODIS in the tropic is large, and in the mid-latitude, it is the same.

The effective particle radius is sensitive to radiance of IR4. This result can especially know an excellence in mid-latitude that technology (Choi et al. 2007) separates thermal component and surface reflectance component from IR4 radiance observed in our algorithm.

Up to this point, this paper has compared our products with MODIS. To realize the properties of the final algorithm, it needs to compare the basic product with the final product. In Fig. 8, when comparing the dotted and solid lines, the frequency of thin clouds with an optical thickness below 4 decreases through the decoupling method, instead of the frequency of thick clouds increases. Also in Fig. 9, the frequency of clouds with small particle effective radius below 10 decreases, and the

frequency of clouds with large particles increase. Cloud optical thickness for clouds between 1 and 9 is very important in tropic energy budget balance. Therefore, if clouds of this kind are changed by the decoupling method, the radiative effect of clouds and estimation must be changed. Since the final product has a value closer to MODIS for the basic product, it is obvious that decoupling method with increasing the accuracy of cloud optical thickness and effective particle radius, contribute to increase comprehension for radiative effect of cloud.

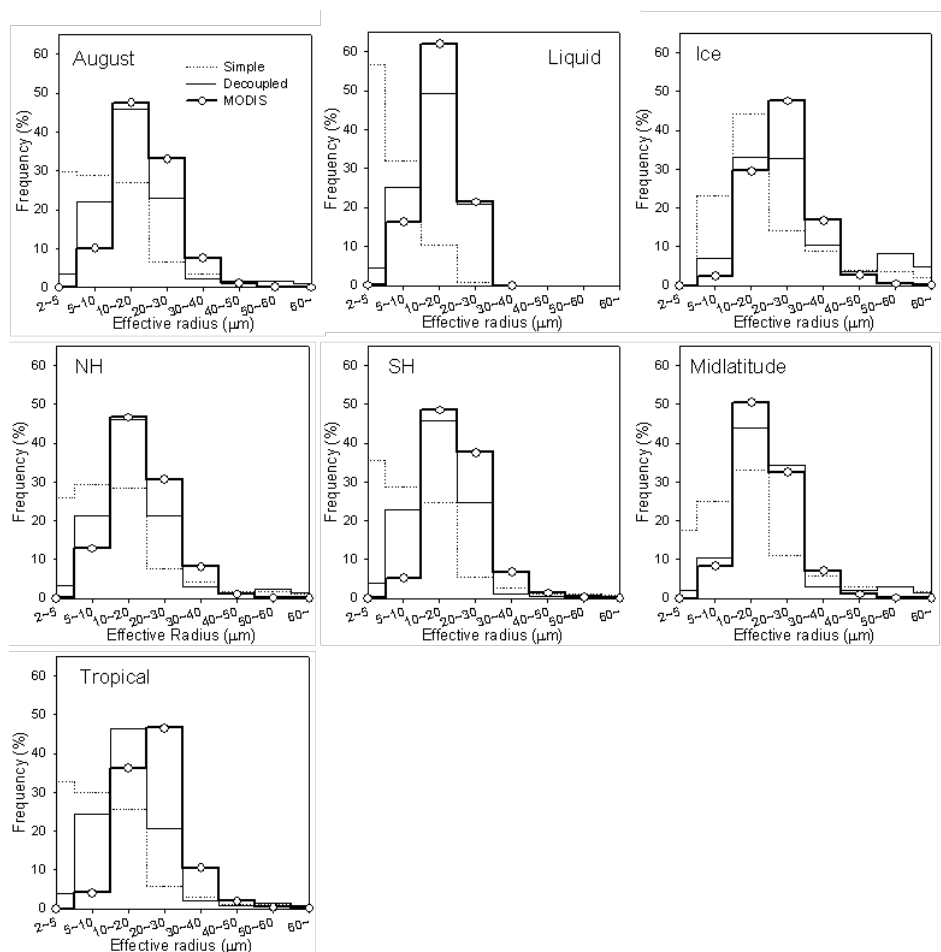


Fig. 9. Same as figure 8 but for cloud effective radius (in μm).

3) Time-series comparison

Climate data comparison provides important information for validation, but it does not show the practical correspondence with MODIS product. This section analyzed the time-series of product for

the nine areas of interest. The hourly average MTSAT product calculated for 1° pixel is compared with the gridded MODIS MOD08 data, because it is retrieved in a hourly 4km resolution. MODIS/Terra pass at 10:30am for all regions. Therefore, hourly MTSAT data does not exactly coincide with MODIS data and time. This can only identify every hour variation and a similar diurnal variation.

Cloud optical thickness and effective particle radius is retrieved when the satellite zenith angle is below 60° . Therefore basic product (a) and final product (b) is only retrieved in the daytime with five areas of interest (Figure 10 and 11). The final product is closer to MODIS data for the basic product.

This improvement is not concerned with the region due to the decoupling method. However, hourly variability of cloud optical thickness and effective particle radius is very big. This is due to the influence of the sun zenith angle on the calculation. Closer to sunrise and sunset, errors increase.

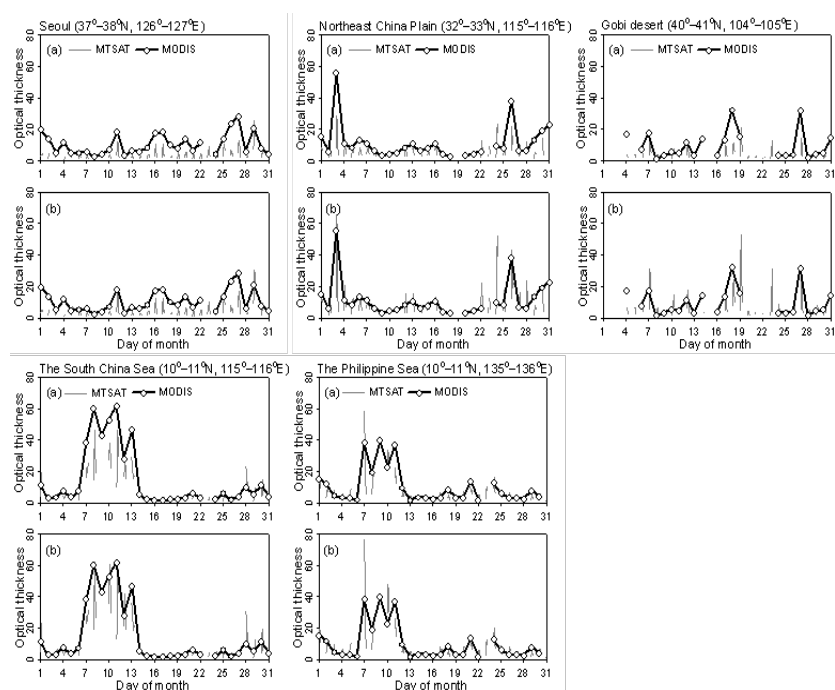


Fig. 10. Same as fig 8 but for base COT using the VIS and IR4 radiances (a), and final COT corrected using the decoupling method in order to have a reflected component from clouds only in the radiances (b).

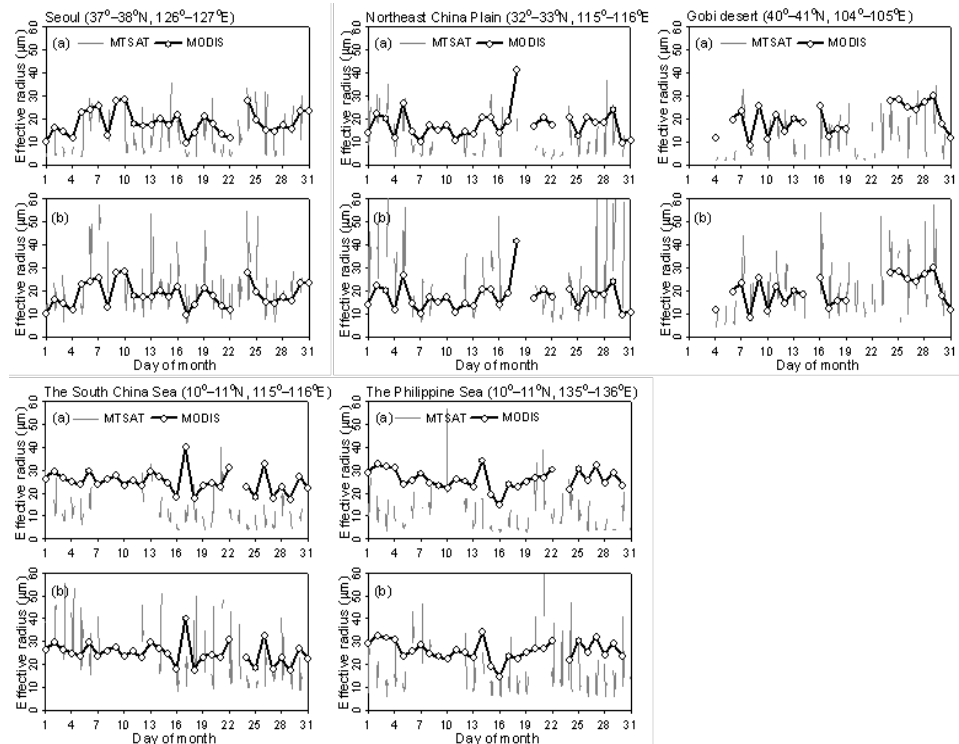
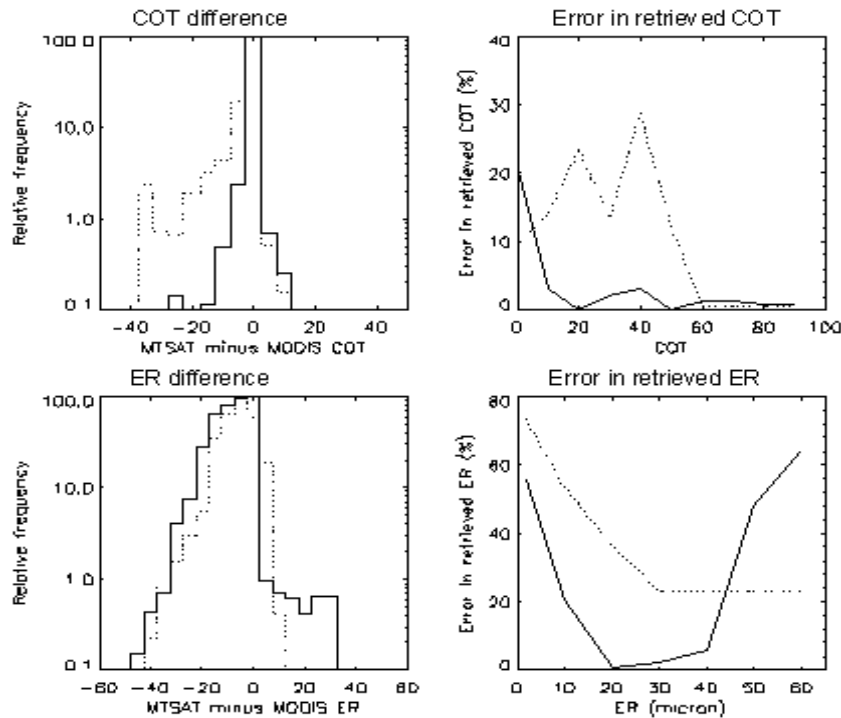


Fig. 11. Same as fig 9 but for base ER (a) and final ER (b).

4) pixel comparison

Fig. 12 shows the results of pixel comparison of cloud information from MTSAT and MODIS. The figure presents relative frequency for the maximum value of the difference between the two products, and errors in MODIS data. Errors were described in the ratio between MTSAT minus MODIS and MODIS product.

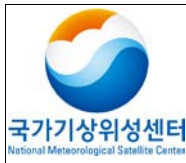
Fig. 12. Relative frequency of MTSAT minus MODIS COT/ER for the maximum values. Errors in the retrieved COT/ER (in %) with respect to the corresponding parameters. The solid and dotted lines indicate values from the final (corrected) and base (uncorrected) products, respectively.



The final cloud optical thickness and MODIS product is within ± 5 . Only 2% of total pixels have a discrepancy with MODIS cloud optical thickness and this error amount decreased noticeably for basic cloud optical thickness. Both basic and final cloud optical thickness is small for clouds above 60 optical thickness. This is contrary to reveal that optical thickness has more errors for thick clouds by physical reason as noted in Choi et al. (2007). More detailed analysis shows the occurrence of very thick cloud is a rare occurrence in nature. Temporal and spatial discrepancy errors are always inherent. We can accidentally see a low error in processing of pixel comparison.

Unlike cloud optical thickness, the final effective particle radius shows a great difference for the value of MODIS. This discrepancy presents for a respectable amount of pixels. It is probably caused by large particles above effective radius $40\mu\text{m}$. IR4 radiance for large particles is less sensitive, it is less the estimated accuracy. A reliable effective particle radius retrieved from MTSAT can appear to be less than $40\mu\text{m}$.

4 Interpretation method of retrieval results



**Algorithm Theoretical
Basis Document
For Cloud Optical Thickness**

Code:NMSC/SCI/ATBD/COT
Issue:1.0 Date:2012.12.26
File: COP-ATBD_V4.0.hwp
Page : 1/43

The reflectance of VIS $0.65\mu\text{m}$ and SWIR $3.75\mu\text{m}$ has a range of 0~100%. LUT is calculated using the Santa Barbara DISORT Atmospheric Radiative Transfer (SBDART) Radiative Transfer Model on the condition of surface albedo. Surface information and scene analysis results are also inputted. We retrieve the cloud optical thickness and effective particle radius using this method. The value of cloud optical thickness has a range of 0~64. Prec. and Acc. are 1.

Table 3. Detailed Output data for the COT algorithm.

OUTPUT DATA								
Parameter	Mnemonic	Units	Min	Max	Prec	Acc	Res	To
Cloud Optical thickness	cld_opt	-	0	128	1	1	Pixel	COT
Effective Cloud Radius	eff_cld_rad	-	0	64	1	1	Pixel	ER

5. COMS version and algorithm improvement after COMS satellite launch

Cloud optical thickness near land with code error in the program is highly retrieved. It occurred the discrepancy in the land and ocean. We modified the code as below. LUT value using cloud optical thickness is composed in case of $R=0$ and $R=0.5$. The COT algorithm requires a difference of radiance in case of $R=0$ and $R=1$. It use to multiply by 2 for scaling (CMDPS final reports, Fig. 2.12.32). The actual code calculates the squared value instead of multiplying by 2. It has a higher value, and the discrepancy occurred (Fig. 13)

```

229
230 |-----
231 | Radiance decoupling
232 |-----
233 | Remove thermal component at 3.7um
234
235 |         cla_rad_swir(i,j) = a*((radiance(i,j)%ir1)**2) + b*radiance(i,j)%ir1 + c
236 |         cla_rad_swir(i,j) = a * (radiance(i,j)%ir1*radiance(i,j)%ir1) + &
237 |             b * radiance(i,j)%ir1 + c
238
239 |         cla_rad_swir_tmp(i,j) = radiance(i,j)%swir - cla_rad_swir(i,j)
240
241 |         cla_rad_vis_tmp(i,j) = radiance(i,j)%vis
242
243 |         vissr(:) = albedo(i,j)*(lut2(:)-lut0(:))*2
244 |         swirsr(:) = albedo(i,j)*(lut3(:)-lut1(:))*2
245 |         vissr(:) = albedo(i,j)*(lut2(:)-lut0(:))*(lut2(:)-lut0(:))
246 |         swirsr(:) = albedo(i,j)*(lut3(:)-lut1(:))*(lut3(:)-lut1(:))
247

```

Fig. 13. Modified COT code for removing land-sea discontinuities

After modified the code, the discrepancy is removed. The result is the same as Fig. 14. High land values are removed instead of COT values, it can see to retrieve well without discontinuity in ocean.

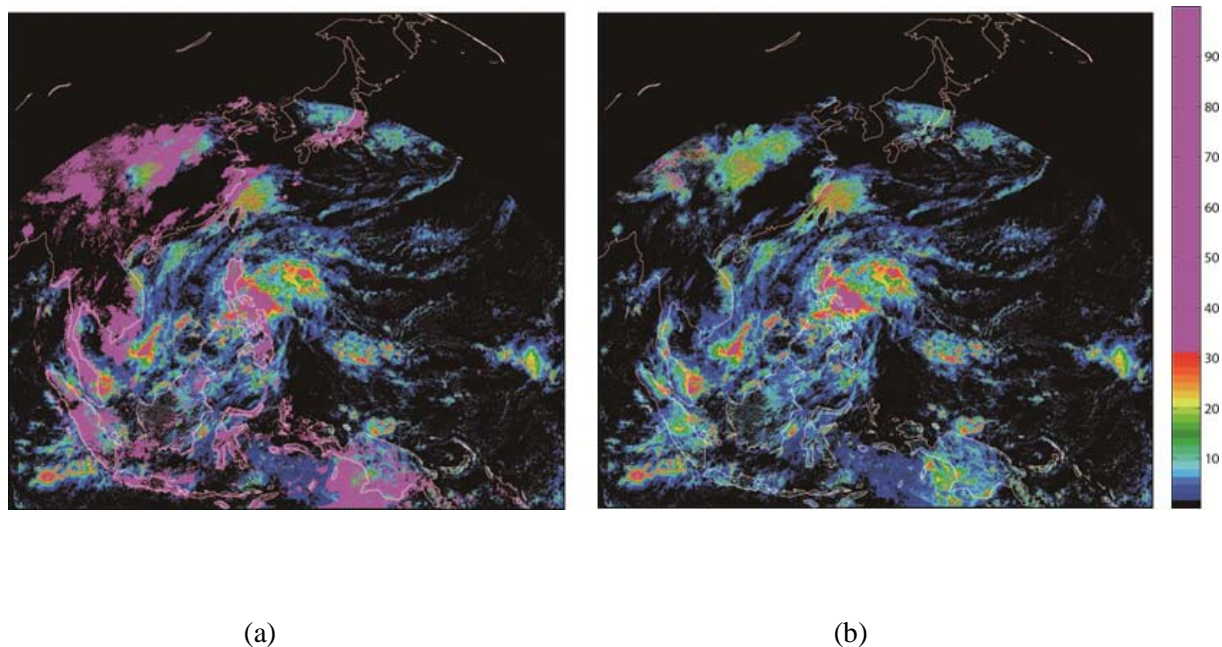
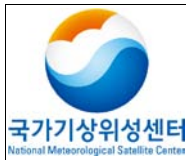


Fig. 14. Cloud optical thickness (a)before and (b)after correcting program code at 15th, Nov, 2011.

6. Problems and possibilities for improvement



**Algorithm Theoretical
Basis Document
For Cloud Optical Thickness**

Code:NMSC/SCI/ATBD/COT
Issue:1.0 Date:2012.12.26
File: COP-ATBD_V4.0.hwp
Page : 1/43

We have to improve the insertion of the quality test code (Table 4) in the standard code, contingency plan code, etc.

Table 4. Quality test result for the COT algorithm.

Quality test result			
Parameter	bit	Value	Meaning
cloud optical thickness	5	from 0 up to 64; step: 1	undefined
effective cloud radius	5	from 0 up to 32; step: 1	undefined
describe COMS input data	2	0	undefined
		1	all useful COMS channel available
		2	at least one useful COMS channel available
define illumination and viewing conditions	3	0	undefined
		1	night
		2	twilight
		3	day
		4	sunlint
describe the quality of the processing itself	2	0	non processed
		1	good quality
		2	poor quality
		3	bad quality

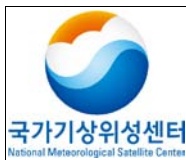


Algorithm Theoretical
Basis Document
For Cloud Optical Thickness

Code:NMSC/SCI/ATBD/COT
Issue:1.0 Date:2012.12.26
File: COP-ATBD_V4.0.hwp
Page : 1/43

7. References

- Baum, B.A., Yang, P., Heymsfield, A.J., Platnick, S., King, M.D., Hu, Y.X. and Bedka, S.T., 2005, Bulk scattering properties for the remote sensing of ice clouds. Part II: Narrowband models. *Journal of Applied Meteorology*, 44, pp. 1896–1911.
- Choi, Y.-S., Ho, C.-H. and Sui, C.-H., 2005, Different optical properties of high cloud in GMS and MODIS observations. *Geophysical Research Letters*, 32, L23823, doi:10.1029/2005GL024616.
- Choi, Y.-S. and Ho, C.-H., 2006, Radiative effect of cirrus with different optical properties over the tropics in MODIS and CERES observations. *Geophysical Research Letters*, 33, L21811, doi:10.1029/2006GL027403.
- Choi, Y.-S., Ho, C.-H., Ahn, M.-H. and Kim, Y.-M., 2007, An exploratory study of cloud remote sensing capabilities of the Communication, Ocean and Meteorological Satellite (COMS) Imagery. *International Journal of Remote Sensing*, 28, pp. 4715-4732.
- Kim, J.-H., Ho, C.-H., Lee, M.-H., Jeong, J.-H. and Chen, D., 2006, Large increase in heavy rainfall associated with tropical cyclone landfalls in Korea after the late 1970s. *Geophysical Research Letters*, 33, L18706, doi:10.1029/2006GL027430.
- King, M.D., Tsay, S.C., Platnick, S.E., Wang, M. and Liou, K.N., 1997, Cloud retrieval algorithms for MODIS: optical thickness, effective particle radius, and thermodynamic phase. In *MODIS Algorithm Theoretical Basis Document (NASA)*.
- King, M.D., Platnick, Hubanks, P.A., Arnold, G.T., Moody, E.G., Wind, G., and Wind, B., 2006, Collection 005 Change Summary for the MODIS Cloud Optical Property (06_OD) Algorithm. Available online at: modis-atmos.gsfc.nasa.gov/C005_Changes/C005_CloudOpticalProperties_ver311.pdf.
- Liou, K.N., 2002, *An introduction to atmospheric radiation* 2nd ed.. Academic Press, San Diego.
- Menzel, W.P., Smith, W.L. and Stewart, T.R., 1983, Improved cloud motion wind vector and altitude assignment using VAS. *Journal of Climate and Applied Meteorology*, 22, pp. 377–384.
- Menzel, W.P., Frey, R.A., Baum, B.A. and Zhang, H., 2006, Cloud top properties and cloud phase algorithm theoretical basis document, In *MODIS Algorithm Theoretical Basis Document, NASA*.
- Nakajima, T.Y. and King, M.D., 1990, Determination of the optical thickness and effective particle radius of clouds from reflected solar radiation measurements, Part 1: Theory. *Journal of the*



Algorithm Theoretical
Basis Document
For Cloud Optical Thickness

Code:NMSC/SCI/ATBD/COT
Issue:1.0 Date:2012.12.26
File: COP-ATBD_V4.0.hwp
Page : 1/43

Atmospheric Sciences, 47, pp1878-1893.

Nakajima, T.Y. and Nakajima, T., 1995, Wide-area determination of cloud microphysical properties from NOAA AVHRR measurement for FIRE and ASTEX region. *Journal of the Atmospheric Sciences*, 52, pp. 4043-4059.

Platnick, S., King, M.D., Ackermann, S.A., Menzel, W.P., Baum, B.A., Riedi, J.C. and Frey, R.A., 2003, The MODIS cloud products: Algorithms and examples from Terra. *IEEE Transactions on Geoscience and Remote Sensing*, 41, pp. 456-473.

Rossow, W.B. and Garder, L.C., 1993a, Cloud detection using satellite measurements of infrared and visible radiances for ISCCP. *Journal of Climate*, 6, pp. 2341–2369.

____ and _____, 1993b, Validation of ISCCP cloud detections. *Journal of Climate*, 6, pp. 2370–2393.

____, Walker, A.W. and Garder, L.C., 1993, Comparison of ISCCP and other cloud amounts. *Journal of Climate*, 6, pp. 2394–2418.

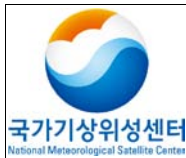
____ and Schiffer, R.A., 1999, Advances in understanding clouds from ISCCP. *Bulletin of the American Meteorological Society*, 80, pp. 2261–2287.

Shupe, M.D., Matrosov, S.Y. and Uttal, T., 2006, Arctic mixed-phase cloud properties derived from surface-based sensors at SHEBA. *Journal of the Atmospheric Sciences*, 63, pp. 6977-11.

Strabala, K.I., Ackerman, S.A. and Menzel, W.P., 1994, Cloud properties inferred from 8–12- μ m data. *Journal of Applied Meteorology*, 33, pp. 212–229.

Yang, P., Zhang, L., Hong, G., Nasiri, S.L., Baum, B.A., Huang, H.L., King, M.D. and Platnick, S., 2007, Differences between collection 4 and 5 MODIS ice cloud optical/microphysical products and their impact on radiative forcing simulations. *IEEE Transactions on Geoscience and Remote Sensing*, 45, pp.2886–2899.

Verlinde, J. and Coauthors, 2007, The mixed-phase arctic cloud experiment. *Bulletin of the American Meteorological Society*, 88, pp. 2052-21.



Algorithm Theoretical
Basis Document
For Cloud Optical Thickness

Code:NMSC/SCI/ATBD/COT
Issue:1.0 Date:2012.12.26
File: COP-ATBD_V4.0.hwp
Page : 1/43

International Journal of Remote Sensing
Vol. 28, No. 21, 10 November 2007, 4715–4732



**An exploratory study of cloud remote sensing capabilities of the
Communication, Ocean and Meteorological Satellite (COMS) imagery**

Y.-S. CHOI†, C.-H. HO*†, M.-H. AHN‡ and Y.-M. KIM†

†Climate Physics Laboratory, School of Earth and Environmental Sciences, Seoul
National University, Seoul 151–742 Korea

‡Meteorological Research Institute, Korea Meteorological Administration, Seoul,
Korea

(Received 8 February 2006; in final form 24 January 2007)

The present study documents optimal methods for the retrieval of cloud properties using five channels (0.6, 3.7, 6.7, 10.8 and 12.0 μm) that are used in many geostationary meteorological satellite observations. Those channels are also to be adopted for the Communication, Ocean and Meteorological Satellite (COMS) scheduled to be launched in 2008. The cloud properties focused on are cloud thermodynamic phase, cloud optical thickness, effective particle radius and cloud-top properties with specific uncertainties. Discrete ordinate radiative transfer models are simulated to build up the retrieval algorithm. The cloud observations derived from the Moderate-resolution Imaging Spectroradiometer (MODIS) are compared with the results to assess the validity of the algorithm. The preliminary validation indicates that the additional use of a band at 6.7 μm would be better in discriminating the cloud ice phase. Cloud optical thickness and effective particle radius can also be produced up to, respectively, 64 and 32 μm by functionally eliminating both ground-reflected and cloud- and ground-thermal radiation components at 0.6 and 3.7 μm . Cloud-top temperature (pressure) in ± 3 K (± 50 hPa) uncertainties can be estimated by a simple 10.8- μm method for opaque clouds, and by an infrared ratioing method using 6.7 and 10.8 μm for semitransparent clouds.

1. Introduction

Clouds are of continual interest because they provide a visible indication of what is going on in the atmosphere. Clouds play an important role in the Earth's climate and could be a crucial factor in evaluating the strength of global warming (see, for example, Lindzen *et al.* 2001, Hartman and Michelsen 2002, Choi *et al.* 2005a, Choi and Ho 2006). Knowledge of such a role requires development of the observational techniques applied to precise satellite measurements. Remote sensing of cloud properties has been studied focusing largely on the applications of the spectral bands of onboard radiometers. In the past few years, cloud analysis techniques have been considerably improved with the advent of Moderate-resolution Imaging Spectroradiometer (MODIS) instruments. The MODIS provides information on a variety of cloud properties by using spectral radiances at 36 visible and infrared (IR) bands (King *et al.* 1997, Baum *et al.* 2000). The detection of cirrus clouds has been particularly enhanced in MODIS by incorporating a band at 1.38 μm , which lies in

*Corresponding author. Email: hoch@cpl.snu.ac.kr

4720

Y.-S. Choi et al

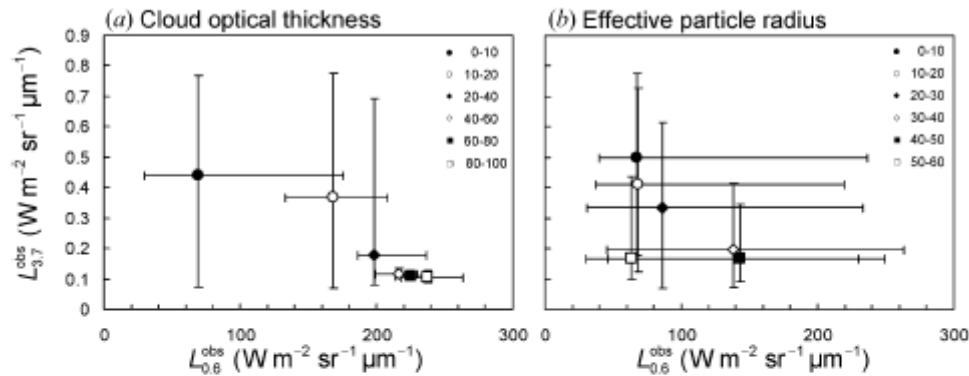


Figure 2. MODIS-retrieved cloud optical thickness (a) and effective particle radius (b) with respect to both 0.6- and 3.7- μm radiance taken from the MODIS observations. The error bars designate the minimum or maximum radiance for the corresponding τ_c and r_e .

content was set to 0.2 (0.02) g m^{-3} . In figure 1(a), ice clouds can have $\text{BTD}_{8.7-10.8}$ greater than about zero regardless of their effective radius, while water clouds cannot. This is consistent with the results of Baum *et al.* (2000) (see their figure 2). Likewise, ice clouds have $\text{BT}_{6.7}$ less than 239 K, whereas water clouds have $\text{BT}_{6.7}$ above 239 K (figure 1(b)). This difference in relation to values of $\text{BT}_{6.7}$ between water and ice clouds can be used to discriminate the cloud phase. $\text{BT}_{10.8}$ of 290 K and $\text{BT}_{6.7}$ of 240 K are maximal values corresponding to the cloud-free scene ($\tau_c=0$) under the specific conditions: the T_g ($=293$ K), ground albedo ($A_g=0.1$) and the profiles of mid-latitude summer. To clarify the values of $\text{BT}_{10.8}$ and $\text{BT}_{6.7}$ as seen from the satellite, we further investigated the MODIS data collected in this study.

The relationships between cloud phase and $\text{BTD}_{8.7-10.8}$, $\text{BT}_{10.8}$ and $\text{BT}_{6.7}$ were examined by using the MODIS data. The relationship between the MODIS cloud phase and $\text{BTD}_{8.7-10.8}$ (or $\text{BT}_{10.8}$) is of course discrete because it is an ice or water phase in those tests. Clouds identified as being in the ice phase have a $\text{BTD}_{8.7-10.8}$ above 0.5 K (or a $\text{BT}_{10.8}$ below 238 K). This study also noted a relationship between the MODIS cloud phase and $\text{BT}_{6.7}$, which is also clear but not as distinct as that with $\text{BTD}_{8.7-10.8}$ (or $\text{BT}_{10.8}$) (data not shown here). Ice clouds identified by the MODIS algorithm tend to have a $\text{BT}_{6.7}$ up to about 250 K. Note that clouds identified as water and mixed phases can also have a $\text{BT}_{6.7}$ between 234 K and 250 K. Consequently, all the types of cloud phases in the MODIS data appear to take similar values of $\text{BT}_{6.7}$ between 234 K and 250 K.

Based on the results of both the RT calculation and the examination of the MODIS data, the algorithm for the cloud phase was recomposed, as described in table 2. The algorithm consists of the phase criteria from ice to unknown phase. The $\text{BT}_{10.8}$ and $\text{BTD}_{10.8-12.0}$ tests are applied from the IR trispectral method of the MODIS. The $\text{BT}_{6.7}$ test is combined with the $\text{BT}_{10.8}$ (or $\text{BTD}_{10.8-12.0}$) test at each

Table 2. The criteria for determining cloud phase.

Ice	Mixed	Water
$\text{BT}_{10.8} < 238$ K or $\text{BTD}_{10.8-12.0} \geq 4.5$ K or $\text{BT}_{6.7} < 234$ K	For no ice $238 \text{ K} \leq \text{BT}_{10.8} < 268$ K or $234 \text{ K} \leq \text{BT}_{6.7} < 250$ K	For no ice/mixed $\text{BT}_{10.8} \geq 285$ K or $\text{BT}_{6.7} \geq 250$ K

represents minimum (maximum) values for water (ice) clouds. The cloud water (ice)

stage of phase decision (table 2). In detail, cloud pixels pass the stage of the ice phase decision first. At this stage, the three tests judge whether the pixel is composed of ice particles or not. If the pixel is not identified as ice, it passes on to the next tests using $BT_{10.8}$ and $BT_{6.7}$ for the mixed phase. If the pixel does not satisfy the criteria of being in the mixed phase, it will go through to the next stage using $BT_{10.8}$ and $BT_{6.7}$ for the water phase. Finally, the pixel unclassified as any phase category will be assigned to an unknown phase.

An effect of missing an 8.7- μm band in the IR trispectral method of the MODIS can be found by comparison of the MODIS cloud phase with that which has been newly retrieved by a $BT_{8.7}$ -free algorithm (i.e. only using 10.8 and 12.0 μm). Table 3 shows that a large portion of the ice clouds are not well distinguished by the $BT_{8.7}$ -free algorithm; the MODIS ice phase takes 40.8% of the total clouds whereas that from the $BT_{8.7}$ -free algorithm takes only 15.6%. Moreover, the MODIS ice phase is in less agreement with that from the $BT_{8.7}$ -free algorithm (15.6% in table 3). More than half of the scenes identified as ice clouds in MODIS are distinguished as mixed phases in the $BT_{8.7}$ -free algorithm (21.2% vs. 40.8% in table 3).

The effect of adding a 6.7- μm band to the $BT_{8.7}$ -free algorithm was also examined in a similar manner, and the results are presented in parentheses in table 3. It can be seen that the MODIS ice phase pixels are easily detected in the $BT_{6.7}$ algorithm (i.e. using 6.7, 10.8 and 12.0 μm). Specifically, MODIS data on detection of ice pixels are in 29.6% agreement with those from the $BT_{6.7}$ algorithm, which takes 72.5% of the total MODIS ice phase. The total percentage of ice phase increased up to 32.5%. This is a considerable improvement compared to the results from the previous $BT_{6.7}$ -free algorithm. Those results account for the fact that large cloud regions comprising ice particles can be identified more accurately by their low $BT_{6.7}$ values, although cloud phases over the regions are not distinguishable through the $BT_{10.8}$ and $BTD_{10.8-12.0}$ threshold tests. Thus, detection of the ice phase using only $BT_{10.8}$ and $BT_{12.0}$ can cause serious problems in that a large portion of such ice clouds can be overlooked. To summarize, we have demonstrated that the 6.7- μm band can be a useful alternative in the case of a missing 8.7- μm band.

4. Cloud optical thickness (τ_c) and effective particle radius (r_e)

Since the determination of the scaled τ_c using a nonabsorbing visible wavelength 0.6- μm band was introduced by King (1987), the method has been used operationally for GMS-5 (Okada *et al.* 2001). τ_c is solely retrieved by this method because the near-IR channel is not available. Here, GMS-5 assumed the effective particle radius

Table 3. Comparison of cloud phase from the MODIS IR trispectral algorithm and from the algorithm for the COMS, as described in table 2. The numbers (in parentheses) designate those from the algorithm from which $BT_{6.7}$ is excluded (included).

COMS	MODIS					
	Clear	Water	Mixed	Ice	Uncertain	Total
Clear	13.0	0.0	0.0	0.0	0.0	13.0
Water	0.0	11.5 (19.7)	0.0	0.1 (0.3)	0.9 (4.1)	12.5 (24.1)
Mixed	0.0	2.3 (2.2)	7.1 (5.5)	21.2 (8.4)	5.8 (5.1)	36.4 (21.2)
Ice	0.0	0.0 (0.3)	0.0 (1.6)	15.6 (29.6)	0.0 (1.0)	15.6 (32.5)
Uncertain	0.0	13.8 (3.9)	0.0	3.9 (2.5)	4.9 (2.9)	22.6 (9.3)
Total	13.0	27.7	7.1	40.8	11.5	100.0

- Spectrometer (MODIS). *IEEE Transactions on Geoscience and Remote Sensing*, **30**, pp. 2–27.
- KING, M.D., TSAY, S.C., PLATNICK, S.E., WANG, M. and LIU, K.N., 1997, Cloud retrieval algorithms for MODIS: optical thickness, effective particle radius, and thermodynamic phase. In *MODIS Algorithm Theoretical Basis Document* (NASA).
- LE GLEAU, H., 2005, *Software User Manual of the SAFNWC/MSG: Scientific Part for the PGE01-02-03. SAFNWC Software V1.2*. Available online at: <http://www.meteorologie.eu.org/safnwc/publis.htm>, pp. 35–53. Meteo, France.
- LINDZEN, R.S., CHOU, M.D. and HOU, A.Y., 2001, Does the earth have an adaptive infrared iris? *Bulletin of the American Meteorological Society*, **82**, pp. 417–432.
- MCCLATCHEY R.A., FENN, R.W., J. SELBY, E.A., VOLZ, F.E. and GARING, J.S., 1972, *Optical Properties of the Atmosphere*, 3rd edn. AFCRL Environment Research Paper No. 411, (Bedford, Massachusetts: Cambridge Research Laboratory), p. 108.
- MENZEL, W.P., SMITH, W.L. and STEWART, T.R., 1983, Improved cloud motion wind vector and altitude assignment using VAS. *Journal of Climate and Applied Meteorology*, **22**, pp. 377–384.
- MENZEL, W.P., BAUM, B.A., STRABALA, K.I. and FREY, R.A., 2002, Cloud top properties and cloud phase. In *MODIS Algorithm Theoretical Basis Document* (NASA), ATBD_MOD_04, NASA Goddard Space Flight Center. Available online at: http://modis-atmos.gsfc.nasa.gov/MOD06_L21.
- NAKAJIMA, T.Y. and KING, M.D., 1990, Determination of the optical thickness and effective particle radius of clouds from reflected solar radiation measurements, Part 1: Theory. *Journal of the Atmospheric Sciences*, **47**, pp. 1878–1893.
- NAKAJIMA, T.Y. and NAKAJIMA, T., 1995, Wide-area determination of cloud microphysical properties from NOAA AVHRR measurements for FIRE and ASTEX regions. *Journal of the Atmospheric Sciences*, **52**, pp. 4043–4059.
- OKADA, I., TAKAMURA, T., KAWAMOTO, K., INOUE, T., TAKAYABU, Y. and KIKUCHI, T., 2001, Cloud cover and optical thickness from GMS-5 image data. In *Proceedings GAME AAN/Radiation Workshop*, 8–10 March 2001, Phuket, Thailand (Nagoya: GAME International Project Office), pp. 9–11.
- PAVOLONIS, M.J. and HEIDINGER, A.K., 2004, Daytime cloud overlap detection from AVHRR and VIIRS. *Journal of Applied Meteorology*, **43**, pp. 762–778.
- RICCHIAZZI, P., YANG, S., GAUTIER, C. and SOWLE, D., 1998, SBDART: a research and teaching software tool for plane-parallel radiative transfer in the earth's atmosphere. *Bulletin of the American Meteorological Society*, **79**, pp. 2101–2114.
- SMITH, W.L. and PLATT, C.M., 1978, Comparison of satellite-deduced cloud heights with indications from radiosonde and ground-based laser measurements. *Journal of Applied Meteorology*, **17**, pp. 1796–1802.
- STRABALA, K.I., ACKERMAN, S.A. and MENZEL, W.P., 1994, Cloud properties inferred from 8–12- μm data. *Journal of Applied Meteorology*, **33**, pp. 212–229.
- TAKANO, Y. and LIU, K.N., 1989, Solar radiative transfer in cirrus clouds. Part I: Single scattering and optical properties of hexagonal ice crystals. *Journal of the Atmospheric Sciences*, **46**, pp. 3–19.
- WYLIE, D.P., MENZEL, W.P., WOOLF, H.M. and STRABALA, K.I., 1994, Four years of global cirrus cloud statistics using HIRS. *Journal of Climate*, **7**, pp. 1972–1986.
- KEY, J.R. and INTRIERI, J.M., 2000, Cloud particle phase determination with the AVHRR. *Journal of Applied Meteorology*, **39**, pp. 1797–1804.
- KEY, J.R., 2002, *Steamer Version 3.0 User's Guide* (Madison, WI: NOAA/NESDIS). Available online at: stratus.ssec.wisc.edu.
- KING, M.D., 1987, Determination of the scaled optical thickness of clouds from reflected solar radiation measurements. *Journal of the Atmospheric Sciences*, **44**, pp. 1734–1751.
- KING, M.D., KAUFMAN, Y.J., MENZEL, W.P. and TANRE, D., 1992, Remote sensing of cloud, aerosol, and water vapor properties from the Moderate Resolution Imaging